Lattice 2026 at the University of Maryland, USA

Portraits of Charmoniumlike States from Lattice QCD

Speaker: Dr. Geng Li

Co-authors: Qingyang Liu, Xiangyu Jiang, Ying Chen, Chunjiang Shi, Wei Sun

ligeng@ihep.ac.cn, qyliu@ihep.ac.cn, cheny@ihep.ac.cn

July 31, 2026

Institute of High Energy Physics (IHEP), Chinese Academy of Sciences (CAS)

Based on: arXiv:2505.21193

中国科学院高能物理研究所
Institute of High Energy Physics
Chinese Academy of Sciences

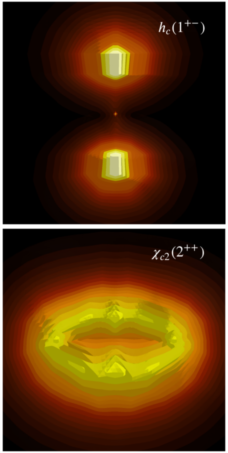

Answering Three Questions

1. What does a meson (charmonium $c\bar{c}$) look like inside?

2. How important are relativistic effects in charmonium?

3. What is the $c\bar{c}$ distribution inside a hybrid $c\bar{c}g$?

Density–density correlation

Meson interpolators: $O_H^{(i)} = \bar{c}\,\Gamma_H^{(i)}\,c, \quad i = 3$

$$\eta_c : \gamma_5 \quad J/\psi : \gamma_i \qquad h_c : \ \epsilon_{ijk}\sigma_{jk}$$
$$\chi_{c0} : \mathbf{1} \qquad \chi_{c1} : \gamma_5\gamma_i \quad \chi_{c2} : |\epsilon_{ijk}|\gamma_j D_k$$

Density operator: normal-ordered charm-number density

$$\rho(\vec{x}) = [:\bar{c}\gamma_4 c:](\vec{x}) = [:c^\dagger c:](\vec{x}).$$

Density–density correlation

For a hadron at rest, probe the equal-time relative separation:

$$C_H(\vec{r}) = \langle H|\rho(\vec{0})\,\rho(\vec{r})|H\rangle.$$

Wave-function interpretation

Neglect $c\bar{c}$ annihilation and treat the pair as $c\bar{c}'$:

$$C_H(\vec{r}) = \int d^3\vec{x}\,|\Phi_c(\vec{x})|^2|\Phi_{c'}(\vec{x}-\vec{r})|^2.$$

Lattice calculation

$$\boxed{C_H(\vec{r}) \approx \frac{C^{(4)}(t_1, t; \vec{r})}{C_H^{(2)}(t_1)}}$$

source → insertion → sink: $0 \to t \to t_1$

$t = t_1/2, \quad t_1/a_t = 24,\ 48$

$N_f = 2$, ~ 400 cfgs, $N_S^3 \times N_T = 16^3 \times 128$

$a_s/a_t \simeq 5$, $a_s = 0.136(2)$ fm, $m_\pi \simeq 420$ MeV

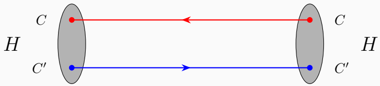

two-point function $C_H^{(2)}$

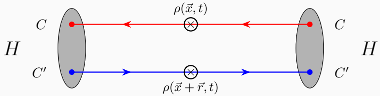

four-point function $C_H^{(4)}$

Charmonium spatial distributions

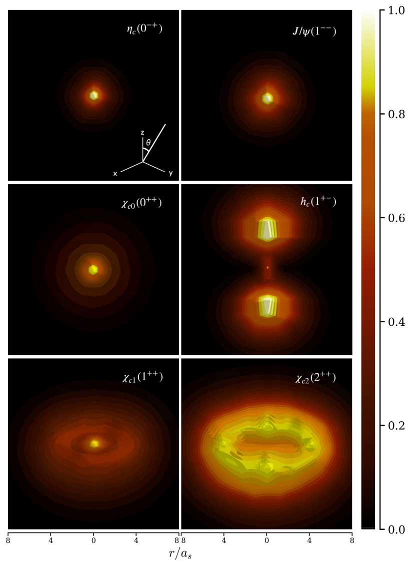

spherical · spindle-shaped · toroidal (doughnut-shaped)

Nonrelativistic L–S coupling $\Longrightarrow J^{PC}$

$$\mathbf{J} = \mathbf{L} + \mathbf{S}, \qquad P = (-1)^{L+1}, \qquad C = (-1)^{L+S}$$

$L\backslash S$	$S = 0$	$S = 1$
$L = 0$	${}^1S_0 : \eta_c(0^{-+})$	${}^3S_1 : J/\psi(1^{--})$
$L = 1$	${}^1P_1 : h_c(1^{+-})$	${}^3P_J : \chi_{cJ}(J^{++}),\ J = 0, 1, 2$

Total distribution: radial part × angular part

$$C_H(\vec{r}) = |\phi_H(r)|^2 |\xi_H(\theta, \phi)|^2,$$

Angular part ξ_H is determined by Clebsch–Gordan coefficients and spherical harmonics Y_{Lm_L}.

$H\ (\lvert J J_z\rangle)$	$\lvert\xi_H(\theta,\phi)\rvert^2$
$\eta_c(\lvert 00\rangle),\ J/\psi(\lvert 10\rangle)$	$\lvert Y_{00}\rvert^2 = \frac{1}{4\pi} \propto \text{const.}$
$\chi_{c0}(\lvert 00\rangle)$	$\frac{1}{3}\sum_{m=-1}^{1} \lvert Y_{1m}\rvert^2 = \frac{1}{4\pi} \propto \text{const.}$
$h_c(\lvert 10\rangle)$	$\lvert Y_{10}\rvert^2 \propto \cos^2\theta$
$\chi_{c1}(\lvert 10\rangle)$	$\lvert Y_{1\pm1}\rvert^2 \propto \sin^2\theta$
$\chi_{c2}((\lvert 22\rangle - \lvert 2,-2\rangle)/\sqrt{2})$	$\lvert Y_{1\pm1}\rvert^2 \propto \sin^2\theta$

Radial distribution

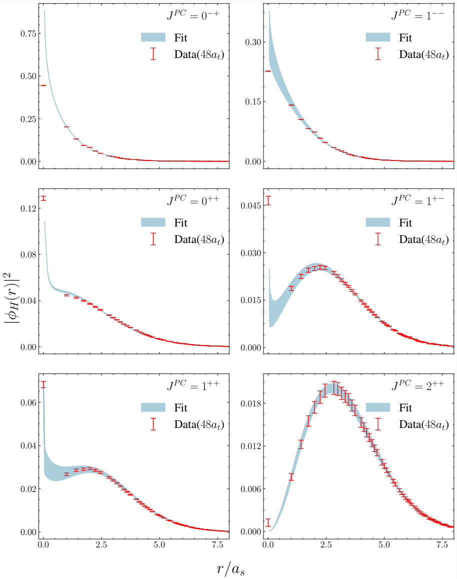

Nonrelativistic expectation

- Radial normalization ($d^3\mathbf{r} = r^2 dr\, d\Omega$):
  $1 = 4\pi \int_0^\infty dr\, r^2 |\phi_H(r)|^2$.
- NRQM bound-state form:

$$\phi_{nL}(r) = r^L f_{nL}(r),\ f_{nL}(0) \neq 0,\ f_{nL}(r \to \infty) \to 0.$$

- r^L controls the origin, $f_{nL}(r)$ the large-r falloff

$$S \text{ wave}: \quad |\phi_{1S}(r)|^2 \underset{r\to 0}{\longrightarrow} \text{const.}, \quad |\phi_{1S}(0)|^2 \neq 0,$$

$$P \text{ wave}: \quad |\phi_{1P}(r)|^2 \underset{r\to 0}{\propto} r^2, \quad |\phi_{1P}(0)|^2 = 0.$$

- Lattice: $|\phi_{h_c,\chi_{c0},\chi_{c1}}(0)|^2 \neq 0$, while $|\phi_{\chi_{c2}}(0)|^2 \approx 0$.
  Pure NRQM fails—relativistic effects are required.
- Relativistic fit: Blue bands are best-fit solutions of the Cornell–Dirac equation.

Panels (top left → bottom right): η_c, J/ψ, χ_{c0}, h_c, χ_{c1}, χ_{c2}.

1. Solve the single-particle Dirac equation in an isotropic Cornell potential model.

$$[\vec{\alpha}\cdot\hat{p} + \beta(\bar{m} + \sigma r)]\,\Psi = \left(E + \frac{\alpha_c}{r}\right)\Psi, \qquad \Psi_{\kappa,m}(\vec{r}) = \begin{pmatrix} F_\kappa(r)\,\chi^{(l)}_{jm}(\theta,\phi)/r \\ iG_\kappa(r)\,\chi^{(l')}_{jm}(\theta,\phi)/r \end{pmatrix}.$$

$l = j - \frac{1}{2}\ (\kappa < 0)$, $\quad l = j + \frac{1}{2}\ (\kappa > 0)$, $\quad l' = 2j - l$: upper/lower orbital angular momenta,

$\kappa = -(l+1)$ (with $j = l + \frac{1}{2}$), $\quad \kappa = l$ (with $j = l - \frac{1}{2}$) : Dirac spin–orbit quantum number.

2. Upper and lower orbital components of each charmonium.

$H(J^{PC})$	κ	j_c	F_κ : upper (l)	G_κ : lower (l')
$\eta_c(0^{-+})$	-1	$\frac{1}{2}$	$S\ (l=0)$	$P\ (l'=1)$
$J/\psi(1^{--})$	-1	$\frac{1}{2}$	$S\ (l=0)$	$P\ (l'=1)$
$\chi_{c0}(0^{++})$	1	$\frac{1}{2}$	$P\ (l=1)$	$S\ (l'=0)$
$h_c(1^{+-})$	$1, -2$	$\frac{1}{2}, \frac{3}{2}$	$P\ (l=1)$	$S\ (l'=0) \oplus D\ (l'=2)$
$\chi_{c1}(1^{++})$	$1, -2$	$\frac{1}{2}, \frac{3}{2}$	$P\ (l=1)$	$S\ (l'=0) \oplus D\ (l'=2)$
$\chi_{c2}(2^{++})$	-2	$\frac{3}{2}$	$P\ (l=1)$	$D\ (l'=2)$

3. The separated radial equation is solved numerically and fits the lattice distributions very well.

$$\begin{pmatrix} \bar{m} + \sigma r - \dfrac{\alpha_c}{r} & -\dfrac{d}{dr} + \dfrac{\kappa}{r} \\ \dfrac{d}{dr} + \dfrac{\kappa}{r} & -\bar{m} - \sigma r - \dfrac{\alpha_c}{r} \end{pmatrix} \begin{pmatrix} F_\kappa \\ G_\kappa \end{pmatrix} = E \begin{pmatrix} F_\kappa \\ G_\kappa \end{pmatrix}.$$

Numerical solutions for F_κ and G_κ

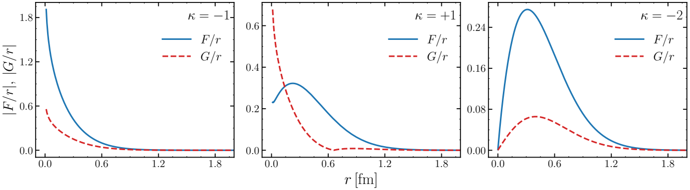

- F_κ: nonrelativistic upper component.
- G_κ: relativistic lower component.
- Near $r = 0$, $|F_\kappa|$ is only a few times $|G_\kappa|$, **relativistic component non-negligible**.

Angular consequence: a quadrupole component

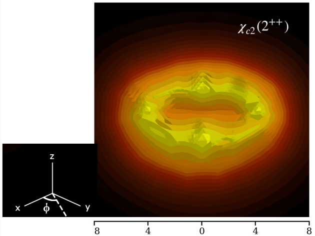

$$|\Psi_{\chi_{c2}}(\vec{r})|^2 = \frac{1}{4\pi r^2}\Big[\tfrac{3}{2}F_{-2}^2(r)\sin^2\theta + \tfrac{5}{2}G_{-2}^2(r)\sin^2\theta(\sin^2\theta\sin^2 2\phi + \cos^2\theta)\Big].$$

Remarkably, the $\sin^2 2\phi$ term produces four additional peaks at $\phi = \frac{\pi}{4}, \frac{3\pi}{4}, \frac{5\pi}{4}, \frac{7\pi}{4}$, giving rise to a quadrupole.

1. Exotic quantum numbers require gluonic degrees of freedom.

A pure $q\bar{q}$ meson obeys $P = (-1)^{L+1}$ and $C = (-1)^{L+S}$; therefore 1^{-+} and 0^{+-} are forbidden.

A charmonium hybrid couples $c\bar{c}$ to an excited gluonic field, schematically $|c\bar{c}g\rangle$.

2. Two representative pictures of hybrid dynamics (schematics by OpenAI Codex).

Core–gluon coupling

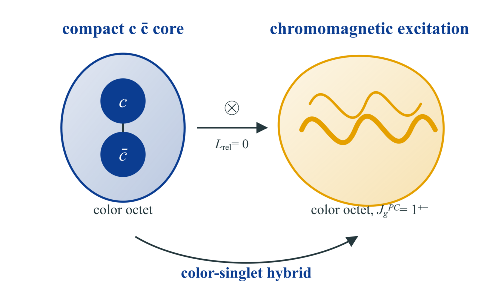

Compact $c\bar{c}(\mathbf{8}_c)$ core $\otimes$ chromomagnetic $1^{+-}(\mathbf{8}_c)$ excitation $\to \mathbf{1}_c$.

Born–Oppenheimer / flux tube

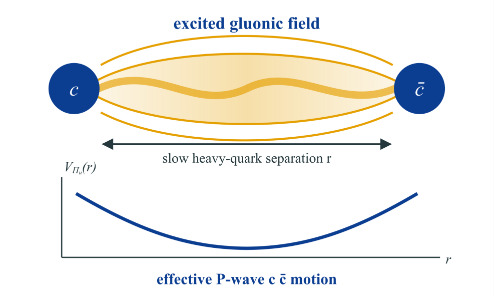

Slow $c\bar{c}$ motion in an excited gluonic BO potential; the simplest 1^{-+} portrait has effective P-wave motion.

Which picture does Nature prefer?

$C_H(\vec{r})$ measures the c–$\bar{c}$ separation, not the full $c\bar{c}g$ size

$\eta_{c1}(1^{-+})$

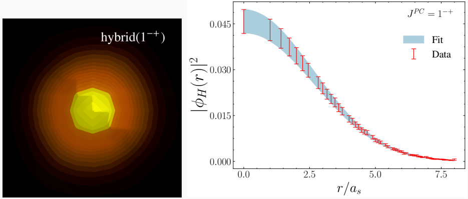

$\sqrt{\langle r^2 \rangle} = 0.58(7)$ fm

$h_{c0}(0^{+-})$

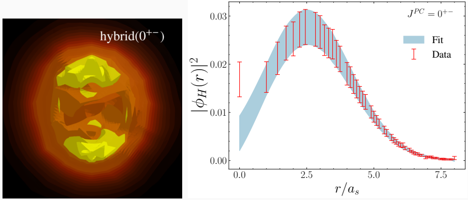

$\sqrt{\langle r^2 \rangle} = 0.59(8)$ fm

Qualitative interpretation

- **Scale comparison:** $1S$: 0.43–0.47 fm | exotic $c\bar{c}$: 0.58–0.59 fm | $1P$: 0.63–0.72 fm.
- **Core–gluon picture:** η_{c1} : $[c\bar{c}(1^{--})] \otimes [g_{\rm mag}(1^{+-})]_{L_{\rm rel}=0}$, h_{c0} : $[c\bar{c}(1^{++})] \otimes [g_{\rm mag}(1^{+-})]_{L_{\rm rel}=0}$. The portraits are compatible with relative S-wave coupling; the h_{c0} assignment is more tentative.
- **Uncertainty:** Higher-state contamination may remain; Affected by statistical fluctuations.
- **Within uncertainties, the core–gluon assignments are favored over the simplest adiabatic BO picture.**

1. **What does a meson (charmonium $c\bar{c}$) look like inside?**
   The first lattice-QCD spatial portraits reveal the expected angular geometries.
2. **How important are relativistic effects in charmonium?**
   Lower Dirac components explain the central enhancement and the quadrupole structure.
3. **What is the $c\bar{c}$ distribution inside a hybrid $c\bar{c}g$?**
   The exotic channels contain compact $c\bar{c}$ subsystems, favoring an S-wave core–gluon picture.
4. **What is the $c\bar{c}$ distribution inside a fully charmed tetraquark $T_{cc\bar{c}\bar{c}}$?** *Coming soon...*
   Previously, in $J/\psi J/\psi$ scattering, we identified an $X(6200)$ 0^{++} virtual-state candidate and an $X(6600)$ 2^{++} resonance candidate (arXiv:2505.23220; arXiv:2505.24213).

Thank you

Polarization choices used for the angular portraits $J/\psi, h_c, \chi_{c1} : |JJ_z\rangle = |10\rangle, \quad \chi_{c2} : (|22\rangle - |2,-2\rangle)/\sqrt{2}.$

Clebsch–Gordan coupling maps each $^{2S+1}L_J$ assignment to an angular density.

$$\xi^{LS}_{JM}(\hat{r}) = \sum_{m_L, m_S} \langle Lm_L, Sm_S | JM\rangle \, Y_{Lm_L}(\hat{r}) \, \chi_{Sm_S}, \qquad W_H(\hat{r}) = \sum_{m_S} |\xi_{H,m_S}(\hat{r})|^2.$$

The resulting projections reproduce the leading lattice shapes.

$$\begin{aligned}
\eta_c(|00\rangle),\ J/\psi(|10\rangle) :\quad & \xi = Y_{00}\chi_{00},\ Y_{00}\chi_{10}, && W = \frac{1}{4\pi};\\
h_c(|10\rangle) :\quad & \xi = Y_{10}\chi_{00}, && W = \frac{3}{4\pi}\cos^2\theta;\\
\chi_{c0}(|00\rangle) :\quad & \xi = \frac{1}{\sqrt{3}}\left(Y_{11}\chi_{1,-1} - Y_{10}\chi_{10} + Y_{1,-1}\chi_{11}\right), && W = \frac{1}{4\pi};\\
\chi_{c1}(|10\rangle) :\quad & \xi = \frac{1}{\sqrt{2}}\left(Y_{11}\chi_{1,-1} - Y_{1,-1}\chi_{11}\right), && W = \frac{3}{8\pi}\sin^2\theta;\\
\chi_{c2}((|22\rangle - |2,-2\rangle)/\sqrt{2}) :\quad & \xi = \frac{1}{\sqrt{2}}\left(Y_{11}\chi_{11} - Y_{1,-1}\chi_{1,-1}\right), && W = \frac{3}{8\pi}\sin^2\theta.
\end{aligned}$$

Thus χ_{c0} is spherical, while the polarized h_c, χ_{c1}, and χ_{c2} retain characteristic anisotropies.

$$|Y_{00}|^2 = \frac{1}{4\pi}, \qquad |Y_{10}|^2 = \frac{3}{4\pi}\cos^2\theta, \qquad |Y_{1,\pm 1}|^2 = \frac{3}{8\pi}\sin^2\theta.$$

The Coulomb term fixes the short-distance power law.

$$\frac{dF_\kappa}{dr} = -\frac{\kappa}{r}F_\kappa + \frac{\alpha_c}{r}G_\kappa, \qquad \frac{dG_\kappa}{dr} = +\frac{\kappa}{r}G_\kappa - \frac{\alpha_c}{r}F_\kappa,$$

$$F_\kappa = ar^s, \quad G_\kappa = br^s : \qquad \begin{pmatrix} s+\kappa & -\alpha_c \\ \alpha_c & s-\kappa \end{pmatrix}\begin{pmatrix} a \\ b \end{pmatrix} = 0 \quad \Longrightarrow \quad s = \sqrt{\kappa^2 - \alpha_c^2}.$$

For $|\kappa| = 1$ the density diverges weakly, but remains integrable.

$$|\Psi_\kappa(\vec{r})|^2 \sim r^{2(s-1)}, \qquad \int_0^\epsilon dr\, r^2 |\Psi_\kappa(r)|^2 \sim \int_0^\epsilon dr\, r^{2s} < \infty.$$

$$|\kappa| = 1 :\ s < 1 \Rightarrow \text{divergent at } r = 0, \qquad |\kappa| = 2 :\ s > 1 \Rightarrow \text{vanishing at } r = 0.$$

The scalar confining term produces a normalizable Gaussian tail.

$$F'_\kappa \simeq \sigma r G_\kappa, \quad G'_\kappa \simeq \sigma r F_\kappa \implies F''_\kappa, G''_\kappa \simeq \sigma^2 r^2 (F_\kappa, G_\kappa) \implies F_\kappa, G_\kappa \propto e^{-\sigma r^2/2}.$$

Supplemental Material: charmonium densities from Dirac spinors

Couple the charm-quark Dirac spinor to the antiquark spin, then sum over spin components.

$$\Psi_{\kappa m}(\vec{r}) = \begin{pmatrix} F_\kappa(r)\,\chi^{(l)}_{jm}/r \\ iG_\kappa(r)\,\chi^{(l')}_{jm}/r \end{pmatrix} \xrightarrow{\langle jm,\frac{1}{2}m_{\bar{c}}|JM\rangle} \Psi_{JM} \xrightarrow{\sum_{s_c,s_{\bar{c}}}|\cdot|^2} |\Psi_H(\vec{r})|^2,$$

$$\begin{pmatrix} \Psi_{h_c} \\ \Psi_{\chi_{c1}} \end{pmatrix} = \begin{pmatrix} 1/\sqrt{3} & -\sqrt{2/3} \\ \sqrt{2/3} & 1/\sqrt{3} \end{pmatrix} \begin{pmatrix} \Xi^{(1/2)} \\ \Xi^{(3/2)} \end{pmatrix}.$$

The lower components G_κ modify both the central behavior and the angular structure.

$$\mathcal{N}(r) \equiv \frac{1}{4\pi r^2}, \qquad F_\kappa \equiv F_\kappa(r), \quad G_\kappa \equiv G_\kappa(r), \qquad |\Psi_{\eta_c}(\vec{r})|^2 = |\Psi_{J/\psi}(\vec{r})|^2 = \mathcal{N}\left(F_{-1}^2 + G_{-1}^2\right),$$

$$|\Psi_{\chi_{c0}}(\vec{r})|^2 = \mathcal{N}\left(F_1^2 + G_1^2\right),$$

$$|\Psi_{h_c}(\vec{r})|^2 = \mathcal{N}\left[(F_1 - \sqrt{2}F_{-2})^2\cos^2\theta + \frac{1}{3}\{G_1^2 + G_{-2}^2(3\cos^2\theta + 1) + 2G_1G_{-2}(3\cos^2\theta - 1)\}\right],$$

$$|\Psi_{\chi_{c1}}(\vec{r})|^2 = \mathcal{N}\left[(\sqrt{2}F_1 + F_{-2})^2\frac{\sin^2\theta}{2} + \frac{1}{6}\{4G_1^2 + G_{-2}^2(3\cos^2\theta + 1) - 4G_1G_{-2}(3\cos^2\theta - 1)\}\right],$$

$$|\Psi_{\chi_{c2},xy}(\vec{r})|^2 = \mathcal{N}\left[\frac{3}{2}F_{-2}^2\sin^2\theta + \frac{5}{2}G_{-2}^2\sin^2\theta(\sin^2\theta\sin^2 2\phi + \cos^2\theta)\right].$$

Channel-by-channel Cornell–Dirac fits describe the conventional radial distributions.

$$\langle r^2 \rangle = \frac{\int d^3\vec{r}\, r^2 C_H(\vec{r})}{\int d^3\vec{r}\, C_H(\vec{r})}.$$

$H(J^{PC})$	$\bar{m}$ [GeV]	α_c	σ [GeV^2]	$\sqrt{\langle r^2 \rangle}$ [fm]	κ
$\eta_c(0^{-+})$	0.81(2)	0.473(1)	0.083(2)	0.430(6)	−1
$J/\psi(1^{--})$	0.95(8)	0.278(41)	0.087(4)	0.469(8)	−1
$h_c(1^{+-})$	0.50(46)	0.59(10)	0.108(5)	0.666(12)	1, −2
$\chi_{c0}(0^{++})$	0.83(2)	0.688(2)	0.061(2)	0.627(9)	1
$\chi_{c1}(1^{++})$	1.23(16)	0.244(35)	0.089(10)	0.644(10)	1, −2
$\chi_{c2}(2^{++})$	0.73(16)	0.334(65)	0.096(19)	0.717(11)	−2

The RMS radii separate compact $1S$ states from the broader $1P$ states. Dimensional errors include the uncertainty in $a_s = 0.136(2)$ fm.

Supplemental Material: effective-mass systematics

Signal quality sets the usable source–sink separation in each channel.

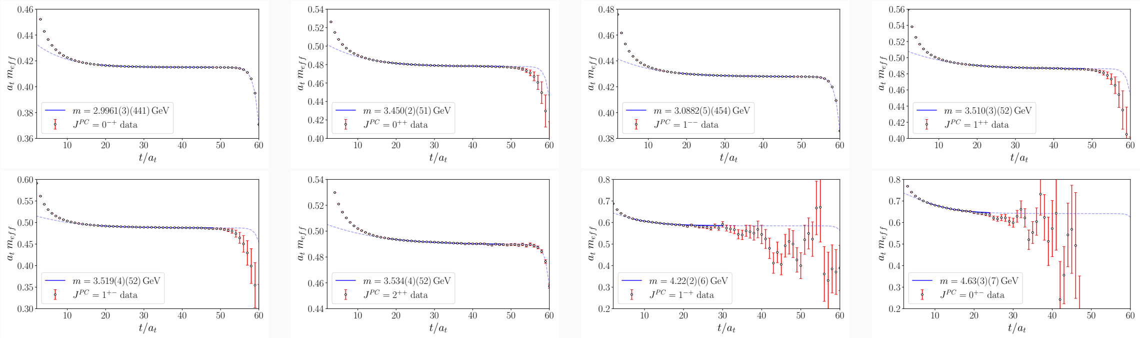

Conventional: use $t_1 = 48a_t$ to reduce excited-state contamination.

Exotic: use $t_1 = 24a_t$ before the signal deteriorates.

Conventional distributions are precise and qualitatively consistent at $t_1 = 24a_t$ and $48a_t$.

Angular portraits

$24a_t$ $48a_t$

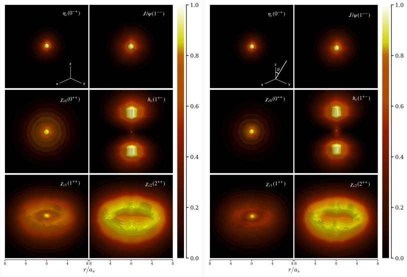

Radial distributions

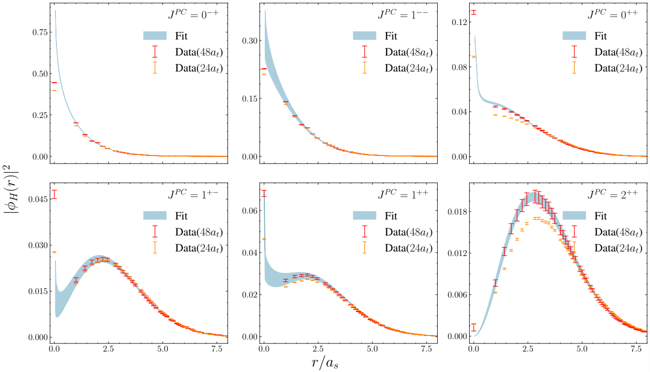

We therefore quote the $48a_t$ results, where excited-state contamination is expected to be smaller.

Supplemental Material: exotic time separation and radial fits

At $48a_t$ the exotic radial errors exceed the central values; only $t_1 = 24a_t$ retains qualitative spatial information.

portrait: $24a_t$ | portrait: $48a_t$ | radial: $24a_t$ | radial: $48a_t$

η_{c1}

h_{c0}

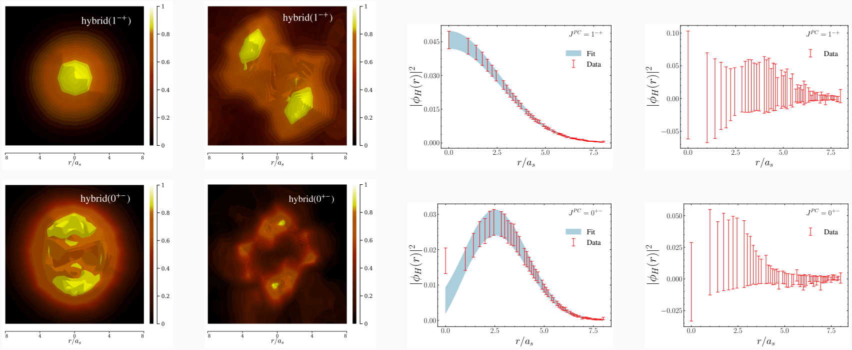

The $24a_t$ profiles admit a common empirical fit.

$$\phi_H(r) = A_H(1 + a_H r)e^{-b_H r^{\omega_H}}.$$

	η_{c1}	h_{c0}
A_H	0.213(9)	0.075(23)
$a_H a_t$	0	0.8(4)
b_H [GeV^2]	0.074(13)	0.082(46)
ω_H	2.05(9)	2.20(27)